NUMERICAL ANALYSIS OF AERODYNAMIC PERFORMANCES OF SINGLE VS. DOUBLE WING (BIPLANE) CONFIGURATION

Jelena Svorcan[1,a], Milica Milić[1,b] and Vladimir Vasić[2,c]

[1]University of Belgrade, Faculty of Mechanical Engineering, Belgrade, Serbia

[2]EDePro, Belgrade, Serbia

[a]jsvorcan@mas.bg.ac.rs, [b]mmilic@mas.bg.ac.rs, [c]vladapobeda@gmail.com

Abstract The number of light aircrafts is constantly increasing and this trend will continue in the future with further development of composite technology and hybrid and purely electric propulsion systems. Since these vehicles enable fast and comfortable transport to destinations in the region and will be employed more and more in urban environments, any improvement of aerodynamic performances together with size reduction would be more than beneficial. Therefore, this paper presents a comparative study of aerodynamic performances of two different configurations of lifting surfaces, single vs. double wing since biplane configuration enables more compact aircraft design. Lift and drag coefficients are obtained by simulating flow by finite volume method in ANSYS Fluent. The flow is considered incompressible and viscous. Reynolds-averaged Navier-Stokes equations are closed by transition SST turbulence model. Results are presented in the form of aerodynamic coefficients of lift and drag as well as flow visualizations by velocity contours. Main observations on aerodynamic performances of biplane wings are presented and discussed.

Keywords: Aerodynamic coefficients; airfoil; CFD; flow separation; turbulence.

1. INTRODUCTION

Up to this year, the number of aircrafts, including light, utility and commercial, has been on the constant increase. However, due to the high cost of aircraft fuel and maintenance, a lot of investigative work still has to be performed in order to improve the aerodynamic performances of modern aircrafts (increase lift, reduce drag or achieve both). On the other hand, the development of composite technology and distributed propulsion systems as well as the idea of urban air traffic that is rapidly gaining popularity instigate further advancement of somewhat less common lifting concepts.

One such, very old conception of biplane wings dates back to the beginning of the 20th century. Its primary advantage is its compactness, i.e. the ability to pack large wing area in a small wingspan that enables low stalling speeds and increased maneuverability [1]. Also, the biplane produces less induced drag in comparison to the equivalent monoplane (of equal span and area) [2] that can be further decreased by winglets (i.e. by box wing). However, in this configuration, lower wing operates in somewhat adverse aerodynamic environment which reduces the overall aerodynamic efficiency. Many theoretical, numerical and experimental studies of biplane geometric parameters (gap and stagger) have been performed in order to achieve the optimum lift-to-drag ratio of the biplane wing [2-6]. Similar ideas applied to wind turbine blades are covered in [7-8] and to supersonic flight in [9-10].

The primary goal of the present study is to numerically explore and compare several biplane configurations to the equivalent monoplane in order to define the optimal solution applicable to light aircrafts. Secondary objectives include quantification of individual contributions of lower and upper wing, respectively, as well as detailed visualization of computed flow fields.

2. GEOMETRIC MODELS

As previously mentioned, two configurations, mono- vs. biplane wings, were modeled, analyzed and compared. Both assumed infinite, rectangular, untwisted wings whose cross-section is the laminar airfoil NACA 65_1-412. This airfoil was chosen for its excellent aerodynamic characteristics [11-12]. Namely, at 3 MRe, it achieves maximal lift coefficient $C_{L,max} = 1.52$ at critical angle-of-attack (AoA) $\alpha_{cr} = 14°$. Its relative thickness is 12%, design lift coefficient $C_{L,des} = 0.4$, minimum drag coefficient $C_{D,min} = 0.0045$, zero-lift angle-of-attack $\alpha_n = -3°$ and lift slope $a = 0.11$ [11].

It is also necessary to clearly describe the geometric parameters used to define the mutual position of lower and upper wing in biplane configuration. Here, the simplest biplane model is assumed. It contains two identical wings at zero incidence (i.e. decalage angle is zero) whose horizontal and vertical distances are stagger s and gap g, respectively, as illustrated in Figure 1. Three different biplane models of relative stagger $s/c = [-0.5, 0, 0.5]$ and constant relative gap $g/c = 0.5$ were considered. Negative value of stagger means the lower wing is located in front of the upper wing.
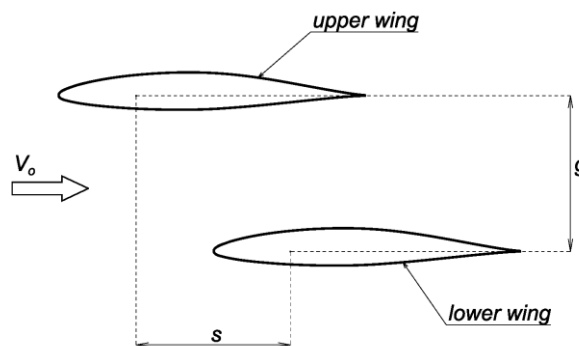

Figure 1. Gap and stagger in biplane configuration where $s/c = 0.5$ and $g/c = 0.5$.

3. NUMERICAL ANALYSIS

3.1. Computational Domain

The chord of the adopted airfoil NACA 65_1-412, located in the center of the assumed xy-coordinate system, is $c = 1$ m. The much larger computational domain stretches around the airfoil(s). It consists of a semi-circle (expanding 10 m fore of the airfoil) and a rectangle (expanding 20 m aft of the airfoil). This size of computational domain allows the application of pressure and velocity values that correspond to the undisturbed flow along its outer boundaries.

3.2. Computational Mesh

All generated numerical meshes are hybrid unstructured. They are both globally and locally refined (particularly in the vicinity of the leading and trailing edges) and contain several layers of thin, prismatic cells around the airfoil walls to accurately capture the flow phenomena appearing in the boundary layer.

In order to ensure the independence of obtained numerical results from the used computational grids, a grid convergence study on a monoplane wing was performed. A family of similar meshes, ranging from extra course to fine, were generated and tried. Table 1 lists their geometric features and total number of cells, while Figure 2 illustrates the convergence of lift and drag coefficients with mesh refinement. Figure 3 provides details of the fine mesh, finally adopted for the remainder of the computation. Corresponding fine meshes generated around biplane wings contain twice as much fluid cells, approximately 125000.

Table 1. Grid parameters.

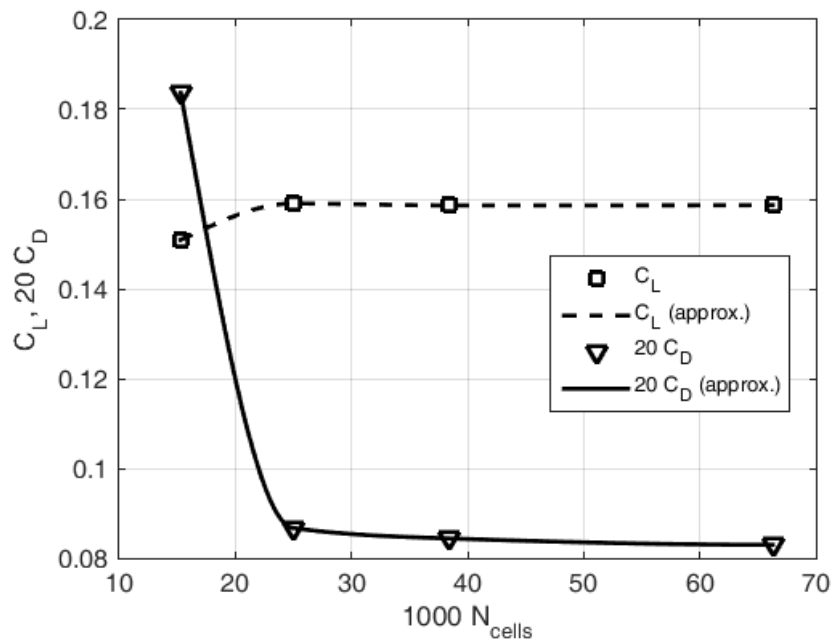| Property	Extra course	Course	Medium	Fine
First layer thickness y_1 (mm)	0.5	0.1	0.05	0.01
Number of prismatic layers N	10	20	30	50
Growth ratio q	1.25	1.2	1.15	1.12
Number of cells along the airfoil suction/pressure side	200	300	400	500
Number of cells along the blunt trailing edge	3	5	10	20
Total number of cells	15290	24940	38414	66269

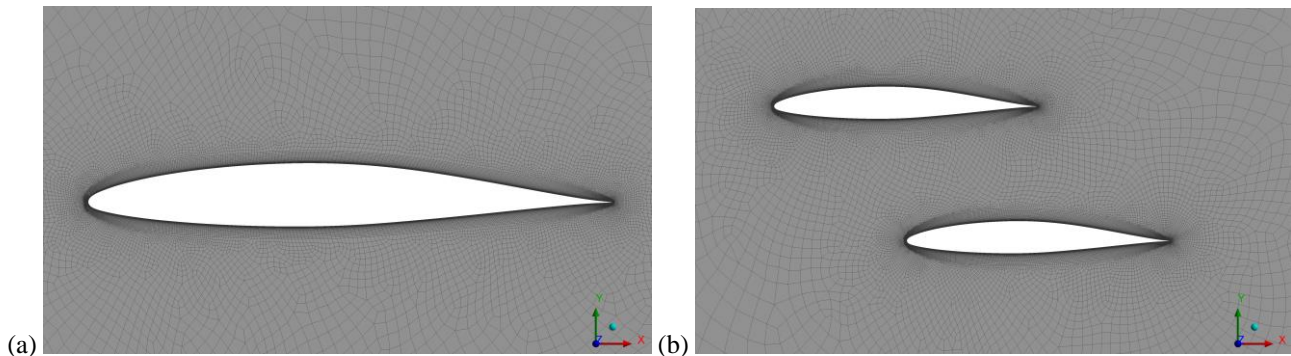**Figure 2. Grid independence study with respect to aerodynamic coefficients.**

(a) (b)

Figure 3. Details of fine computational meshes around: (a) monoplane, and (b) biplane.

3.3. Computational Set-up

Flow computations were realized in engineering software package ANSYS Fluent [13] by finite volume method. Fluid flow was always considered to be steady, planar, incompressible and viscous (transitional or completely turbulent). Reynolds-averaged Navier-Stokes (RANS) equations were closed by the 4-equation transitional shear stress transport (SST) model [13] that enables the resolution of laminar, transitional and turbulent zones appearing around the laminar airfoil NACA 65_1-412.

Velocity vector of the undisturbed flow is defined along the inlet boundary. The assumed speed results in Reynolds number of 3 MRe. Different angles-of-attack α in the range [0°, 15°] are achieved by changing the direction of the undisturbed flow. Zero gauge pressure is assumed along the outlet.

Reference values used for the computation of aerodynamic coefficients of lift and drag are: length $c = 1$ m, area $A = 1$ m^2, density $\rho = 1.225$ kg/m^3 and velocity $V = 43.822$ m/s. Biplane reference area was also computed as a product of chord length c and unit length (since performed analyses are 2D).

Pressure-based solver with SIMPLEC coupling scheme of pressure and velocity fields was employed. All spatial derivatives are approximated by 2nd order schemes. Computations were performed until reaching the converged values of aerodynamic coefficients, usually 5000-20000 iterations.

4. RESULTS AND DISCUSSION

4.1. Validation of the Adopted Computational Methodology

In the beginning, in order to validate the adopted computational approach, the numerical results obtained on a monoplane wing (i.e. airfoil NACA 65_1-412) were compared to the corresponding measured values available in [11]. Figure 4 illustrates both the numerical and experimental lift and drag curves. Although there are some discrepancies (particularly regarding the zero-lift angle-of-attack that seems higher when computed and effectively translates the lift curve downwards), the correlation can be considered satisfactory. The trend of both lines is well captured, including both the laminar bucket and the stall region.
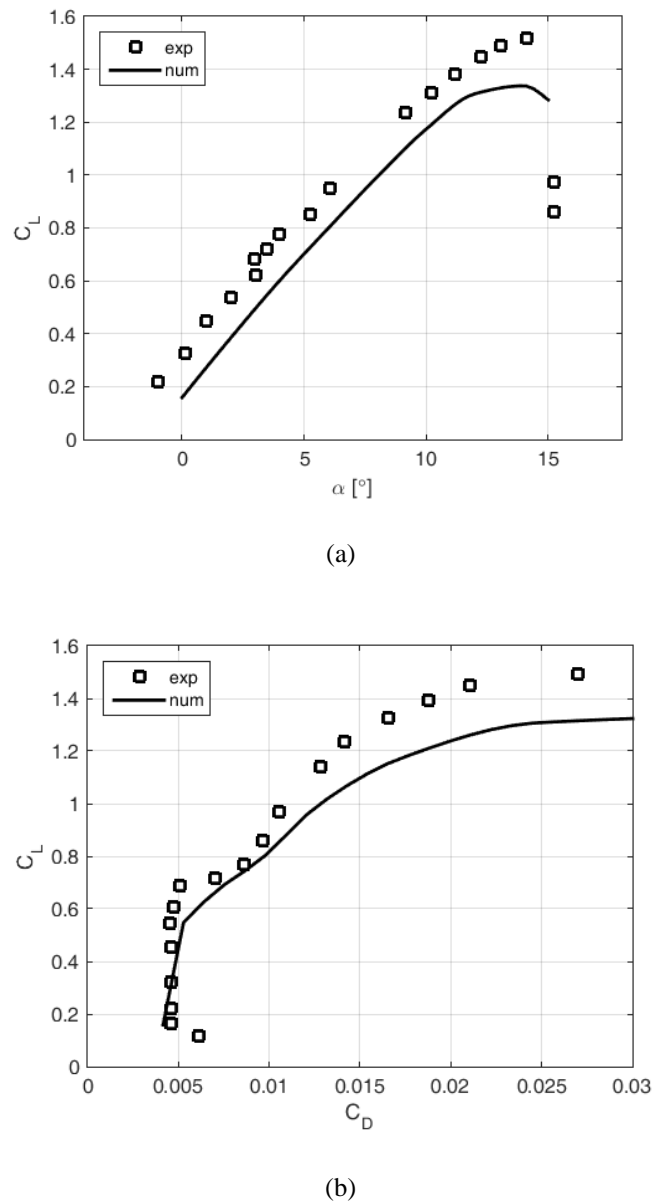
(a)

(b)

Figure 4. Computed vs. measured values of: (a) lift, and (b) drag coefficients on monoplane wing.

4.2. Comparison of Computed Aerodynamic Performances of Different Wings

Aerodynamic coefficients vs. α computed on mono- and biplane wings are illustrated in Figure 5. For comparison, doubled values for monoplane are also depicted since they correspond to biplane wings in terms of the wetted wing surface.

If lift coefficients are compared, it can be noted that performances of biplane wings lie somewhere between the monoplane and doubled monoplane wing (of equal wetted surface). The wing with $s/c = 0.5$ achieves the highest $C_{L,max}$, while the wing with $s/c = -0.5$ performs the worst in stall. Lift slopes of all biplanes are similar and slightly lower than the one obtained on equivalent doubled

monoplane, while zero-lift angle-of-attack α_n decreases with increased stagger resulting in higher lift coefficients at lower AoA. On biplane wings, lift loss happens earlier (due to the stall happening on one of the wings) but less strong in comparison to monoplane where stall effects appear quite suddenly.
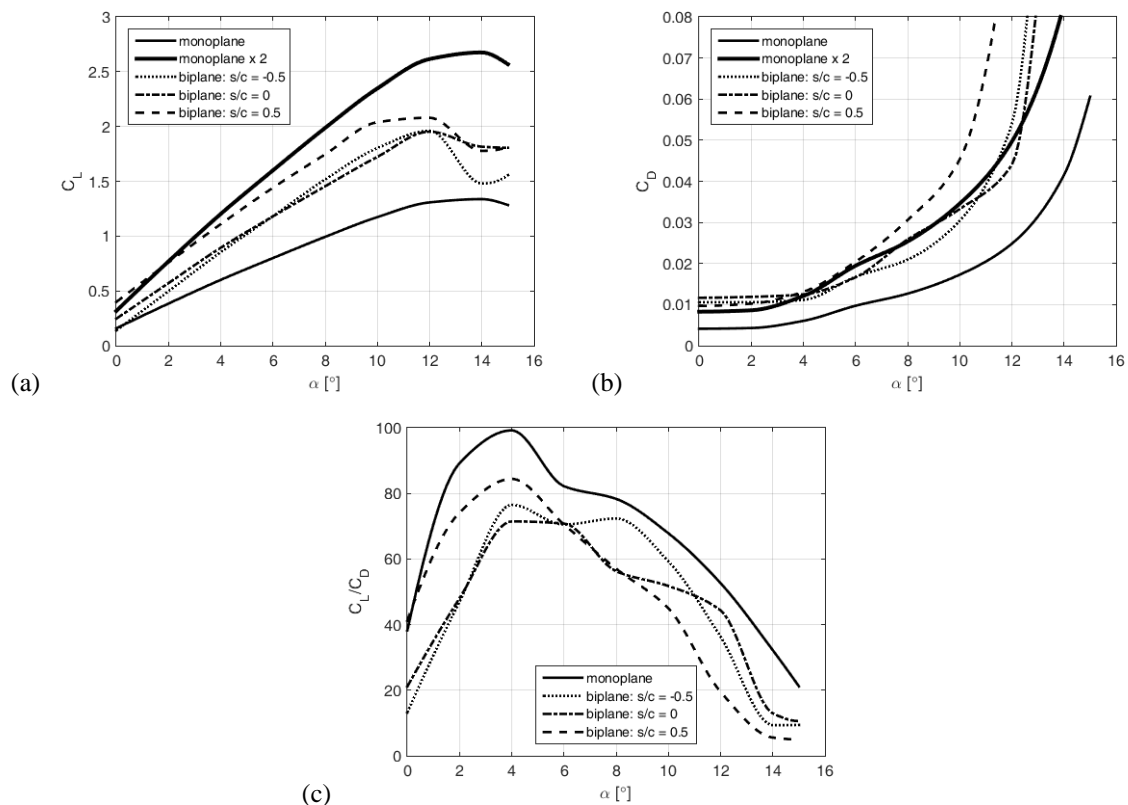

Figure 5. Computed aerodynamic coefficients: (a) lift, (b) drag, and (c) lift-to-drag ratio.

Although slightly higher than on monoplane wing, the values of drag coefficient at low AoA seem quite satisfactory. Even the laminar bucket region seems well preserved. Again, among the biplane wings, the slightest drag is generated by the wing with $s/c = 0.5$ at angles-of-attack $\alpha \leqslant 4°$, while the wing with $s/c = −0.5$ performs the best at $6° \leqslant \alpha \leqslant 10°$. These occurrences (physical arguments why this happens) are depicted in Figures 6 and 7 by velocity contours. Downwash angle from the upper wing increases with stagger keeping the flow on lower wing attached at higher AoA [3]. I.e. at negative stagger, stall happens first on the lower wing, while at positive stagger, stall in the first place originates from the upper wing.

The highest value of aerodynamic efficiency or lift-to-drag ratio of nearly 100 is achieved on monoplane wing at $\alpha = 4°$. The second in line with the value of 85 accomplished at the same angle-of-attack is the wing with $s/c = 0.5$ (i.e. at the highest considered stagger). The lowest L/D is obtained on the wing with $s/c = 0$ implying that both positive and negative values of stagger increase aerodynamic efficiency.
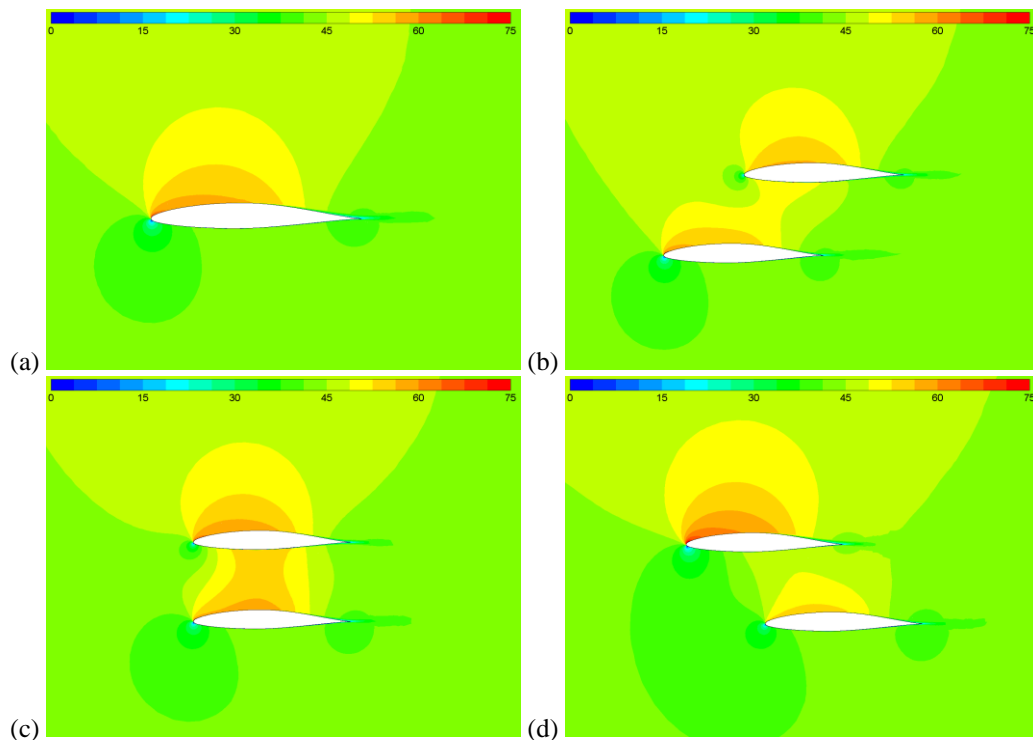
Figure 6. Velocity contours at $\alpha = 4°$ for: (a) monoplane, (b) biplane with $s/c = -0.5$, (c) biplane with $s/c = 0$, and (d) biplane with $s/c = 0.5$.
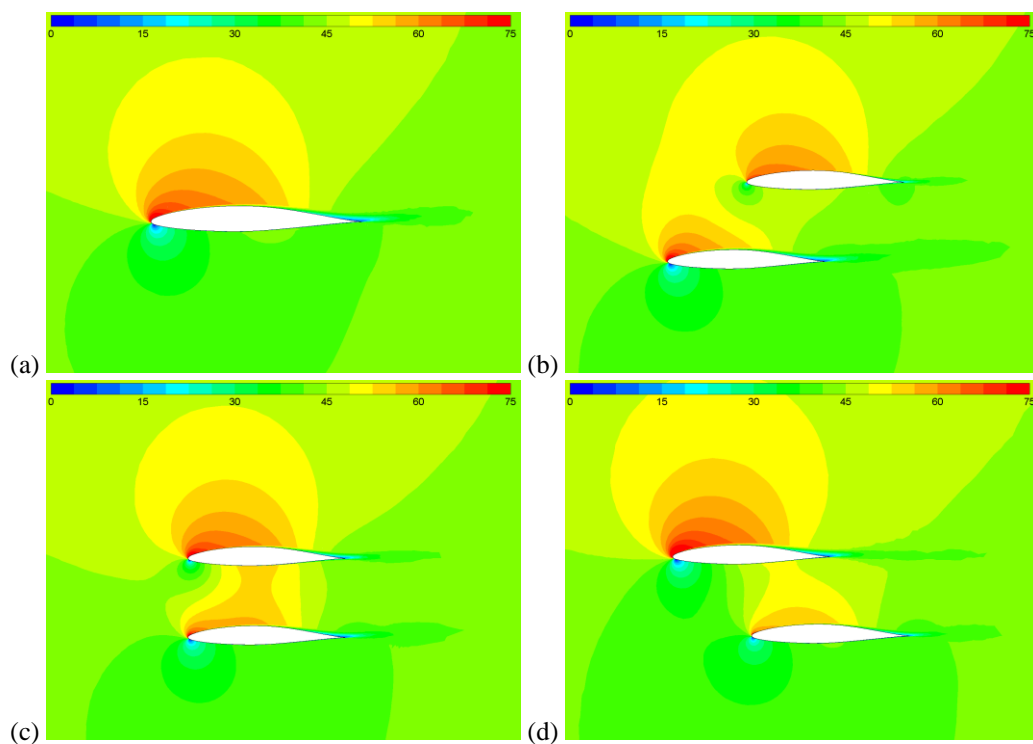

Figure 7. Velocity contours at $\alpha = 8°$ for: (a) monoplane, (b) biplane with $s/c = -0.5$, (c) biplane with $s/c = 0$, and (d) biplane with $s/c = 0.5$.

Division of the aerodynamic load between biplane wings is extremely important for proper flow study as well as subsequent stress analysis. Therefore, relative contributions to lift and drag of the lower wing in biplane configuration are illustrated in Figure 8. Values higher than 100% imply the upper wing produces negative contributions. It can be concluded that at negative and zero stagger lower wing produces significantly more lift at $\alpha \leqslant 12°$. For the same range of angles-of-attack, at positive stagger, the lower wing produces less than 40% of total lift. On the other hand, at negative stagger, the drag coefficient of the lower wing even becomes negative at $\alpha \geqslant 4°$ (which reduces the total drag). The things are vice versa for zero and positive stagger when the lower wing induces the major part of drag force while the upper wing produces negative drag.
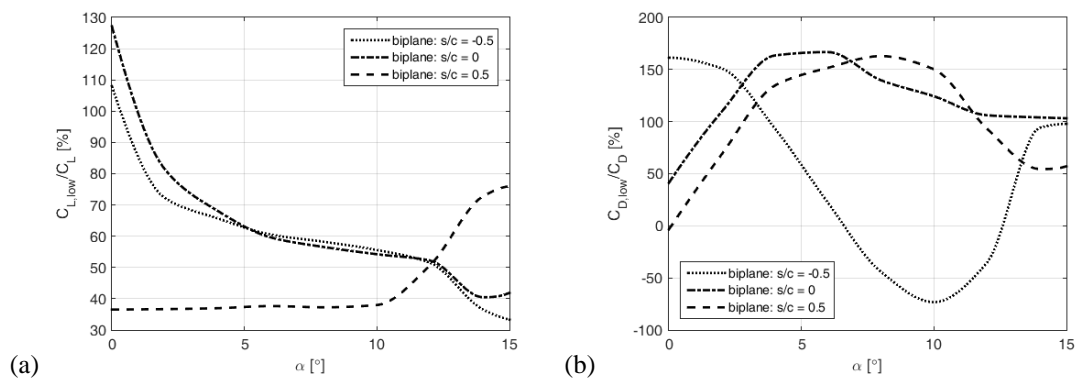

Figure 8. Relative contributions of lower wing in biplane configuration to: (a) lift, and (b) drag.

5. CONCLUSIONS

Planar numerical studies of biplane wings are performed and presented. The effects of stagger are explored in detail. The comparisons in performance to equivalent monoplanes are conducted, after which the following conclusions can be formulated:

- Overall, no biplane configuration can outperform the monoplane wing of equivalent wetted surface (doubled monoplane) with respect to global aerodynamic coefficients. However, the benefits of biplanes are load distribution and compact design,
- The biplane with $s/c = 0.5$ (highest stagger) achieves the highest lift coefficient but at the smallest critical angle,
- From the drag perspective, biplane with $s/c = 0.5$ performs better at lower AoA, while biplane with $s/c = -0.5$ is more appropriate at medium AoA,
- Both positive and negative stagger increases lift-to-drag ratio of biplane wings.

Performed planar studies can be improved by considering 3D effects, more refined spatial and temporal scales, different approaches to resolving turbulence, etc.

Acknowledgements

References

[1] Gudmundsson S., 2014, *General Aviation Aircraft Design: Applied Methods and Procedures*, Butterworth-Heinemann, Oxford.

[2] Gall P., and Smith H., 1987, Aerodynamic Characteristics of Biplanes with Winglets, *Journal of Aircraft*, 24 (8), pp. 518-522.

[3] Kang H., Genco N., and Altman A., 2009, Gap and Stagger Effects on Biplanes with End Plates - Part I. *Proceeding of the 47th AIAA Aerospace Sciences Meeting and Exhibit*, art. no. 2009-1085, AIAA, Orlando.

[4] Kang H., Genco N., and Altman A., 2009, Gap and Stagger Effects on Biplanes with End Plates - Part II. *Proceeding of the 47th AIAA Aerospace Sciences Meeting and Exhibit*, art. no. 2009-1086, AIAA Orlando.

[5] Genco N., and Altman A., 2009, Parametric Study of the Performance of a Biplane Joined at the Tips. *Proceeding of the 47th AIAA Aerospace Sciences Meeting and Exhibit*, art. no. 2009-0206, AIAA, Orlando.

[6] Cai Y., Liu G., Zhu X., Tu Q., and Hong G., 2019, Aerodynamic Interference Significance Analysis of Two-Dimensional Front Wing and Rear Wing Airfoils with Stagger and Gap Variations, *Journal of Aerospace Engineering*, 32 (6), art. no. 04019098.

[7] Chiu P., 2017, Aerodynamics and Optimal Design of Biplane Wind Turbine Blades (PhD thesis), University of California, Los Angeles.

[8] Zhong J., and Li J., 2020, Aerodynamic Performance Prediction of NREL Phase VI Blade Adopting Biplane Airfoil, *Energy*, 206, art. no. 118182.

[9] Maruyama D., Matsushima K., Kusunose K., and Nakahashi K., 2008, Aerodynamic Design of Three-dimensional Low Wave-drag Biplanes Using Inverse Problem Method. *Proceedings of the 46th AIAA Aerospace Sciences Meeting and Exhibit*, art. no. 2008-0289, AIAA, Reno.

[10] Yamazaki W., and Kusunose K., 2014, Biplane-Wing/Twin-Body-Fuselage Configuration for Innovative Supersonic Transport, *Journal of Aircraft*, 51 (6), pp. 1942-1952.

[11] Abbott I., von Doenhoff A., and Stivers L. Jr., 1945, Summary of Airfoil Data (NACA-TR-824), NACA, Langley Field.

[12] Stefanović Z., 2005, *Airfoils*, University of Belgrade, Faculty of Mechanical Engineering, Belgrade.

[13] ANSYS, 2017, ANSYS Fluent Theory Guide (Release 18.1), ANSYS, Inc., Canonsburg.